Generation of Multi-Contact Motions with Passive Joints: Improvement of Sitting Pivot Transfer Strategy for Paraplegics

Sébastien Lengagne, Jovana Jovic, Camilla Pierella, Philippe Fraisse, Christine Azevedo-Coste

Abstract— **In this paper, we present a motion generation method to improve the Sitting Pivot Transfer (SPT) strategy. We propose to analyze the impact of the torque generated on lower limbs by using Functional Electrical Stimulation (FES) on the maximal forces underneath the hands needed for the SPT. This method, based on an optimization process considers a 3D whole body biomechanical model and produces multi-contact motions with desired constant knee torque value. From the generated motions, we study the impact of legs muscle stimulation on the arm forces during the SPT motion. This approach highlights the relationship between the lower limbs stimulation and the maximal forces underneath the hands. The generated motions provide a good tradeoff between the minimization of the maximal hand forces and an excessive increase of the lower limb muscular fatigue.**

Index Terms— **Motion generation, Multi-contact, constant torque, FES, paraplegia.**

INTRODUCTION

After a Spinal Cord Injury (SCI), paraplegic patients are constrained on wheelchairs, and they depend exclusively on their arms for everyday-life activities [1], [2]. The role of Upper Limbs (ULs) changes completely, becoming the primary source of movement: wheelchair propulsion, weight relief, and transfer are some of the new activities that paraplegics have to face. In complement to the arm support, FES can be used to help subject in performing everyday activities. It has been demonstrated that persons with SCI can re-obtain the capability of standing up, standing and walking by means of FES of the lower extremity muscles [3], [4], [5]. The principles of FES consists in placing electrodes on the surface of the skin and in applying series of electrical pulses which generate several chemical reactions and thus lead to muscle contraction. Despite all its advantages, inappropriate FES pattern will cause muscle fatigue and thus unable the patient to perform the task [4]. Moreover, if the lower limbs under FES control are not coordinated with the voluntary controlled body parts, the patient will not be able to maintain its balance and the body will eventually collapse. As a consequence, FES pattern needs to be chosen appropriately.

Many studies show that the upper limbs of wheelchair users are subjected to a greater mechanical stress than healthy people [1], [2], [6], [7], [8]. This additional mechanical stress on shoulder, elbow and wrist joints can cause secondary impairments such as muscle atrophy and impingement. Hence, it leads to really negative consequences on SCI subjects' independence, especially if we take into account that paraplegic patients perform SPT around 15 and 20 times a day [1], [6].

In consequence, the aim of this paper is to investigate the ability of optimization process in combination with 3D whole body biomechanical model to predict optimal SPT trajectories and to evaluate the influence of different types of FES stimulation pattern on the corresponding motion.

In motor control and biomechanics literature, a classical assumption is that human beings perform a motion according to certain optimal criteria, i.e. movement control can be related to a problem of minimizing a biomechanical cost function. Optimization processes have been extensively used to provide a better understanding of human postural and locomotor system [9], [10], [11], [12]. These models are objectively and experimentally assessable because of their quantitative predictions and they are usually used to describe relatively simple tasks involving healthy subjects.

Though the SPT technique is the most commonly used technique by paraplegic subjects to perform transfer from the wheelchair to a target seat and vice versa [13], according to the authors knowledge, no optimization procedure has never been used in this context. However, some works in the robotic fields deal with optimal motion generation for open and closed-loop robotics systems [14]. To generate SPT trajectories, we extend our original method for the generation of multi-contact motions [15], [16] for the HRP-2 Robot. The main technical issue is to compute the contact forces that ensure balance and desired constant joint torques.

In the case of the SPT motion, the identification of the appropriate cost function is still very challenging. This is mainly due to the multi-objective nature of the task, the low intra-inter-subject reliability in the execution of the task, the change in environmental constraints moreover SPT task requires the control of a highly redundant system that can be organized in many ways [1], [2], [6]. In this paper, we consider the cost function as the weigthed sum of joint torques, joint jerks and motion duration, that was used in [16] to produce a smooth and low-energy motion.

Section I introduces the general problem statement, then Section II describes the biomechanical model. Section III is dedicated to the multi-contact forces computation. Finally, Section IV presents the task specific optimization process and the different scenarios, i.e. FES patterns, used for its validation. Results of our optimization process and conclusion are given at the end.

S. Lengagne is with the Karlsruhe Institute of Technology, Institute for Anthropomatics, Humanoids and Intelligence Systems Lab, Adenauerring 2, 76131 Karlsruhe, Germany.

J. Jovic, C. Pierella, P. Fraisse, C. Azevedo-Coste are with INRIA LIRMM/DEMAR, 161 rue Ada, 34392 Montpellier Cedex 5, France.

P. Fraisse is also with the Interactive Digital Human group of the LIRMM, UMR 5506 Université Montpellier II - CNRS, Montpellier, France.

I. Problem statement

To generate a motion, we look for the joint trajectories $q(t)$ over the motion duration T_f that minimizes a cost function C and ensures a set of continuous g,h and discrete z constraints as summarized in:

$$\begin{array}{cc} \underset{q(t)}{\text{argmin}} & C(q(t)) \\ \forall i, \forall t \in [0,T_f] & g_i(q(t)) \leq 0 \\ \forall j, \forall t \in [0,T_f] & h_j(q(t)) = 0 \\ \forall t_k \in \{t_1, t_2, ..., t_n\} & z_k(q(t_k)) \leq 0 \end{array} \tag{1}$$

The problem (1) is called infinte programming problem and is usually turned into a semi-infinite programming one using of a set of parameters $\mathbf{X}$ to compute the joint trajectories:

$$\begin{array}{cc} \underset{\mathbf{X}}{\text{argmin}} & C(\mathbf{X}) \\ \forall i, \forall t \in [0,T_f] & g_i(\mathbf{X},t) \leq 0 \\ \forall j, \forall t \in [0,T_f] & h_j(\mathbf{X},t) = 0 \\ \forall k & z_k(\mathbf{X},t_k) \leq 0 \end{array} \tag{2}$$

In this paper we compute the joint trajetories $q(t)$ using B-Spline basis functions [17]:

$$q_j(t) = \sum_{i=1}^{m} b_i^K(t) p_{j,i} \tag{3}$$

Here, the set of parameters $\mathbf{X} \in \mathbb{R}^n = \{p_{1,1}, \cdots, p_{1,m}, p_{2,1}, \cdots, \beta, T_f\}$ where $p_{j,i}$ is the i^{th} control point of joint j, β a set of parameters as presented in Section III-A and T_f the motion duration. This parametrization was already used in [14] and has the nicety to ensure the joint position and velocity limits by a set of linear constraints on the optimization parameters $\mathbf{X}$. Note that the constraints function g_i, h_j, z_k can rely on any variables of the biomechanical model.

In this paper, we use the method presented in [15] to deal with the continuous inequality and equality constraints g,h. This method is based on a polynomial approximation of the state variables to ensure the constraint satisfaction over the whole motion duration contrary to classical time-grid discretization. Eventually, the solver (we use IPOPT [18]) is able to compute the optimal set of parameters $\tilde{\mathbf{X}}$ that describes the optimal motion according to the biomechanical model presented hereafter.

II. Modeling

In this section, we present all the physical limits we take into account and how to compute them from the joint trajectories.

A. Biomechanical Model

In this paper, we use a simplified model of the human as shown on Figure 1, with 28 degrees of freedom (dof) considering rotoide (R) and spherical (S) joints as presented on Table II-A. For sake of simplicity, we consider revolute and spherical joint for knees and shoulders, even if some more accurate models exist and were used in robotics [19], [20]. Since we are interested into the evolution of the contact forces, we assume that this simplification will not impact our results.

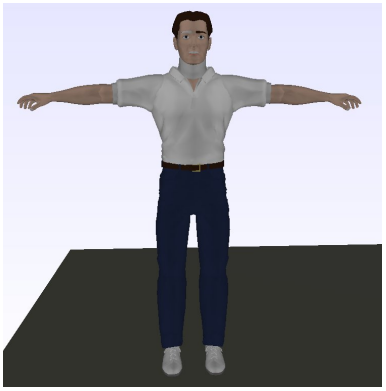

Fig. 1. Representation of the human.

TABLE II-A
Representation of the degrees of freedom of the biomechanical model

Body	Joint type	Number of dof
Torso	S	3
Head	S [1]	3
Shoulder	S	2 × 3
Elbow	R	2 × 1
Forearm	R	2 × 1
Wrist	R	2 × 1
Hip	S	2 × 3
Knee	R	2 × 1
Ankle	S	2 × 3

To ensure the contact position, we set equality constraints between the position and orientation of the frame attached to the given body and the expected ones of the frame attached to the environment as done in [15]. We define the contact forces $\mathbb{F}$ as a set of linear forces attached to the frame body assuming that the z component of the force is normal to the contact surface. Eventually, we get a set of N_f linear contact forces $\mathbb{F} = \{F_1, F_2, \cdots, F_{N_f}\}$.

B. Inverse Dynamic Model

We take into account the dynamic effects by considering the inverse dynamic model:

$$\begin{bmatrix} \Gamma \\ 0 \end{bmatrix} = \begin{bmatrix} \mathbb{D}_1(q,\dot{q},\ddot{q}) \\ \mathbb{D}_2(q,\dot{q},\ddot{q}) \end{bmatrix} + \begin{bmatrix} \mathbf{J}_1^T(q) \\ \mathbf{J}_2^T(q) \end{bmatrix} \mathbb{F} \tag{4}$$

where $\Gamma \in \mathbb{R}^n$ is the vector of the joint torques, $\mathbb{D}_1 \in \mathbb{R}^n$ and $\mathbb{D}_2 \in \mathbb{R}^6$ are the dynamics effects due to the joint trajectories (usually presented as the sum of inertial $\mathbf{M}(q)\ddot{q}$, coriolis and centrifugal $\mathbb{C}(q,\dot{q})$ and gravity $\mathbb{G}(q)$ effects: $\mathbb{D} = \mathbf{M}(q)\ddot{q} + \mathbb{C}(q,\dot{q}) + \mathbb{G}(q)$), $\mathbf{J}_1 \in \mathbb{R}^{n \times 3N_f}$ and $\mathbf{J}_2 \in \mathbb{R}^{6 \times 3N_f}$ the components of the Jacobian matrix and $\mathbf{q} \in \mathbb{R}^n$ is a vector containing the n joint positions (q_i). Equation (4) emphasizes the link between the joint trajectories to the contact forces and the joint torques. Section III-A shows how to compute the contact forces.

[1] We consider the joint of the head with a constant value during the motion, hence they are not included in the optimization process.

C. Balance

Due to the nonplanar contact points, we cannot use classical method such as the zero moment point [21] to characterize the balance of the motion. We rather consider a full-body model of the human, and evaluate the balance by monitoring if the contact wrench sum remains in the contact wrench cone as presented in [22]. Those notions are summarized by the fact that the contact forces must counterpart the dynamic effects of the motion and stay within their friction cone:

$$\forall t \in [0,T_f], \forall i \in \{1,\ldots,N_f\} \quad \left\{ \begin{array}{c} F_i^n(t) > 0 \\ ||F_i^t(t)||^2 \leq \mu_i^2 F_i^n(t)^2 \end{array} \right. \tag{5}$$

where μ_i is the friction coefficient related to contact forces F_i. To summarize, those constraints ensure the no sliding and taking off of the contact points.

III. Contact Forces Computation and constant torques

The main technical contribution of this paper is about the computation of the contact forces that must ensure desired joint torques in order to simulate controlled, uncontrolled and stimulated joints.

A. Force Constraints

In case of multi-contact motions, there is an indetermination for the computation of the contact forces; there is an infinity of different internal forces that lead to an infinity of contact forces and joint torques. In our previous works [15], we presented how to remove this indetermination and to compute the contact forces in case of multi-contact motions for a fully-actuated humanoid robot. In this paper, we extend this method to take into account a set of N_e joint torques that must be constant with an expected value Γ_e. Hence, the contact forces must:

- avoid any unexpected sliding or taking off of any part of the human body in contact with the environment such as presented in (5),
- satisfy the second part of the dynamic equation (4),

$$\mathbb{D}_2 + \mathbf{J}_2^T \mathbb{F} = 0 \tag{6}$$

- produce the expected joint torques $[\Gamma_e]$

$$\forall e \quad [\Gamma_e] = D_{1,e} + \mathbf{J}_{1,e}^T \mathbb{F} \tag{7}$$

where $D_{1,e}$ and $\mathbf{J}_{1,e}^T$ represent the e^{th} component and line of $\mathbb{D}_1$ and $\mathbf{J}_1^T$. Note that our method can not be used only if all the components of $\mathbf{J}_{1,e}^T$ are null. That involves that the corresponding joint must be part of a closed-chain.

B. Force Problem Formulation

To find the contact forces that ensure the (6) and (7), the pseudo inverse of the Jacobian matrix can be used. However, the pseudo inverse will minimize the norm of the contact forces, without any effect on the friction or sliding constraint. We rather consider the contact forces that are the solution to the following problem:

$$\begin{array}{c} \min \frac{1}{2} \sum_i \beta_i (\alpha_i ||F_i^t||^2 + F_i^{n2}) \\ \\ \sum_i \left(\left[\begin{array}{c} \hat{P}_i A_i \\ A_i \end{array} \right] [F_i] \right) + [D_2] = 0 \\ \sum_i (\eta_{e,i} [F_i]) + D_{1,e} - [\Gamma_e] = 0 \end{array} \tag{8}$$

where:

- F_i^t is the tangential components of F_i,
- F_i^n is the normal component of F_i,
- $\hat{P}_i$ the screw operator of the contact position,
- A_i the orientation of the contact,
- $\eta_{e,i} \in \mathbb{R}^3$ is the effect of force $[F_i]$ on joint torque e,
- β_i weight the repartition of the different contact forces,
- α_i weight the tangential components regarding to the normal one for each contact forces.

Note that problems (8) and (2) must not be confused. In fact, problem (8) must be solved during the modeling of the motion. Hence, the cost function of problem (2) does not mimize the contact forces.

The solution to problem (8) exactly counterparts the dynamics effects and produce the expected joint torques Γ_e, while fulfilling as best as possible the constraint of (5). The exact satisfaction of these constraints is ensured by the optimization solver. Note that defining $\forall i \ \beta_i = 1, \ \alpha_i = 1$ is equivalent to solve the pseudo-inverse problem taking into account constraints of (6) and (7). Since the expected torque value is obtained through this computation, there is no need to include constant torque equality constraint in the global optimization problem (2).

C. Analytic solution

The resolution of problem (8) starts by writing the Lagrangian equation:

$$L = \sum_i \left[\begin{array}{c} \beta_i \alpha_i F_{x,i}^2 \\ \beta_i \alpha_i F_{y,i}^2 \\ \beta_i F_{z,i}^2 \end{array} \right] + \left(\begin{array}{c} \sum_i \left[\begin{array}{c} \hat{P}_i A_i \\ A_i \end{array} \right] [F_i] + [D_2] \\ \sum_i [\eta_{e,i}] [F_i] + [D_{1,e} - [\Gamma_e]] \end{array} \right) [\lambda] \tag{9}$$

Here, we assume that the z-axis is the normal direction of the contact forces and define $[\lambda]$ as the vector of the Lagrange multipliers. The optimal solution fulfills the optimality condition:

$$\frac{\partial L}{\partial (F_{\circ,i}, \lambda_j)} = 0 \tag{10}$$

From the derivative with respect to F_i we have:

$$F_i = -\mathbb{W}_i^{-1} \left[\begin{array}{cccc} \hat{P}_i A_i & A_i & \eta_{e,i} \end{array} \right] [\lambda] \tag{11}$$

with $\mathbb{W}_i = \text{diag}(\beta_i \alpha_i, \beta_i \alpha_i, \beta_i)$. The lagrangian multipliers are computed through:

$$[\lambda] = -\Omega^{-1} \left[\begin{array}{c} D_2 \\ D_{1,e} - [\Gamma_e] \end{array} \right] \tag{12}$$

with:

$$\Omega = \sum_i \left(\left[\begin{array}{c} \hat{P}_i A_i \\ A_i \\ \eta_{e,i} \end{array} \right] \mathbb{W}_i^{-1} \left[\begin{array}{ccc} \hat{P}_i A_i & A_i & \eta_{e,i} \end{array} \right] \right) \tag{13}$$

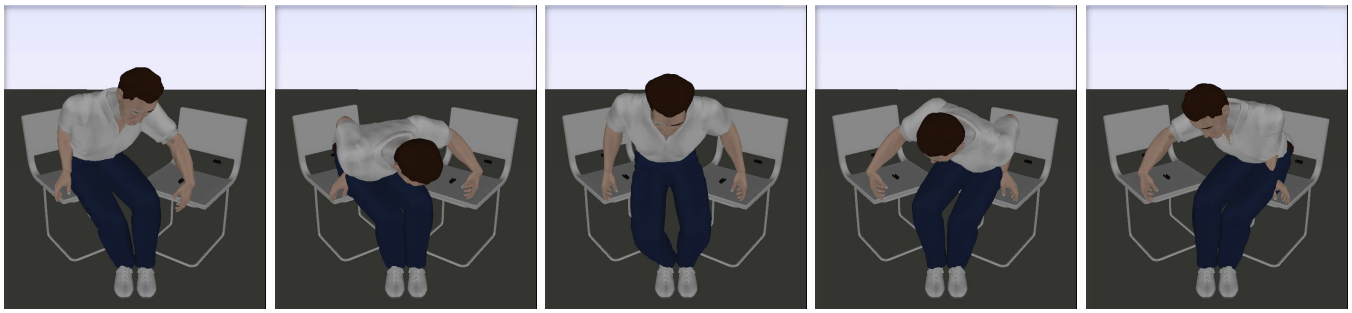

Fig. 2. Screenshots of the SPT Motion. the transfer is performed from the chair on the right to the one on the left of the subject. For this reason, according with the description of the SPT, we call the right arm, trailing arm, and the left arm, leading arm.

where $\Omega \in \mathbb{R}^{(6+N_e)\times(6+N_e)}$ is a $(6+N_e)\times(6+N_e)$ matrix that we easily invert, using, for instance, the Gauss-Jordan algorithm, to find the value of the Lagrange multipliers. Thus, we compute the contact forces from the joint trajectories and using equation (4) we can compute the joint torques.

IV. Optimization Results

A. Sitting Pivot Transfert

Every wheelchair users have their own way to do the SPT using their residual functionalities at the best and according to the environment, but there are common features that characterize the transfer. SPT is divided into three distinct phases:

1) Pre-lift, the preparatory phase which ends when bending forward of the trunk starts;
2) Lift, the phase in which most of the body weight is supported by the upper extremities;
3) Post-lift, the rebalancing phase on the new seat.

Before starting the transfer, individuals usually move their wheelchair as close as possible to the target seat. At first, they move the buttocks forward to the front edge of the seat of wheelchair and, with the help of the arms, place firmly their feet on the floor. Then, they place one hand, called the trailing hand, on a stable position on the wheelchair and the other hand, known as the leading hand, on the target surface far enough to leave sufficient space for the buttocks. From this starting position, subjects bend their trunk forward and sideways, meanwhile they lift up their body and sustain their weight with the arms. After that, with a very rapid twisting motion they place the buttocks on the target seat. The transfer is concluded when the subjects reach again a seated postural stability [7].

Here, we focus only on the lift phase optimization, during which the FES on patients lower limbs should be applied. The starting position is when the back is upon the first chair and the ending position is when the back is upon the second chair as shown on Fig. 2. During this phase both hands are on the handles and both feet are on the ground. The contact positions during the motion are presented in Table IV-A.

We consider the constraint limits as presented in Section II and the objective function in order to minimize a weighted sum of joint torques, jerks and motion duration as presented:

TABLE IV-A
Position and vertical orientation of the contact frames

Contact	X (m)	Y (m)	Z(m)	θ_Z (°)
Right Foot	0	-0.05	0	0
Left Foot	0	0.05	0	0
Right Hand	-0.05	-0.35	0.5	20
Left Hand	-0.05	0.35	0.5	-20
Initial back	-0.2	-0.2	0.4	35
Final back	-0.2	0.2	0.4	-35

$$C(q) = a\int_0^T \sum_i \Gamma_i^2 dt + b\int_0^T \sum_i \dddot{q}_i{}^2 dt + cT \qquad (14)$$

with $a = 1e-2$, $b = 1e-5$ and $c = 4$, are the value we set heuristically to have human like walking motion for the HRP-2 Robot in [16].

B. Scenarios under study:

The complete paraplegic patient with a spinal cord lesion at lumbosacral level is no longer able to control knees and ankles joints, i.e. voluntary production of the joint torque is not possible. In this paper, we consider that our virtual paraplegic patient is not able to voluntary control the knee joints only, while ankle and hip joints are assumed to be active. Future works will adress fully passive legs. The virtually stimulated muscles are quadriceps and biceps femoris. We suppose that those bi-articular muscles produce torque control only at the knee joints. In addition, for the sake of simplicity, we assume that stimulation parameters do not change during the transfer (constant control torque) and that no stimulation leads to a null knee joint torque.

Whole body optimal trajectories for SPT are calculated for seven different scenarios (Sc). The first scenario (Sc 1) represents the behavior of a healthy subject, produces variations of knee joint torque. The others impose a constant value of the knee joint torque (Sc 2: 0 Nm, Sc 3: 10 Nm, Sc 4: 20 Nm, Sc 5: 30 Nm, Sc 6: 40 Nm, and Sc 7: 50 Nm), representing the behavior of a paraplegic subject performing the SPT without (Sc 2) and with (Sc 3-7) FES. Hands and feet positions are the same for all simulations as described in Table IV-A.

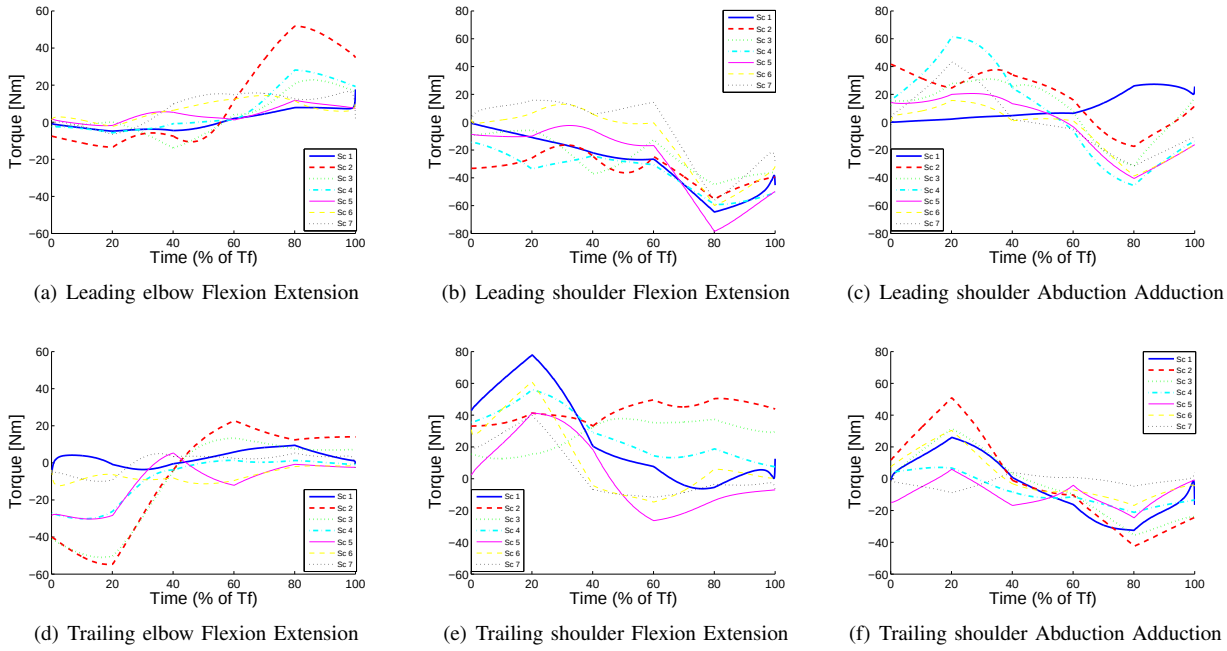

(a) Leading elbow Flexion Extension (b) Leading shoulder Flexion Extension (c) Leading shoulder Abduction Adduction

(d) Trailing elbow Flexion Extension (e) Trailing shoulder Flexion Extension (f) Trailing shoulder Abduction Adduction

Fig. 3. Time history of the torque, espressed as percentage of Tf, for the right and the left arm in different scenarios (Sc). In (c) and (d) positive values correspond to flexion and negative values correspond to extension. In (e) and (f) positive values correspond to adduction and negative values correspond to abduction.

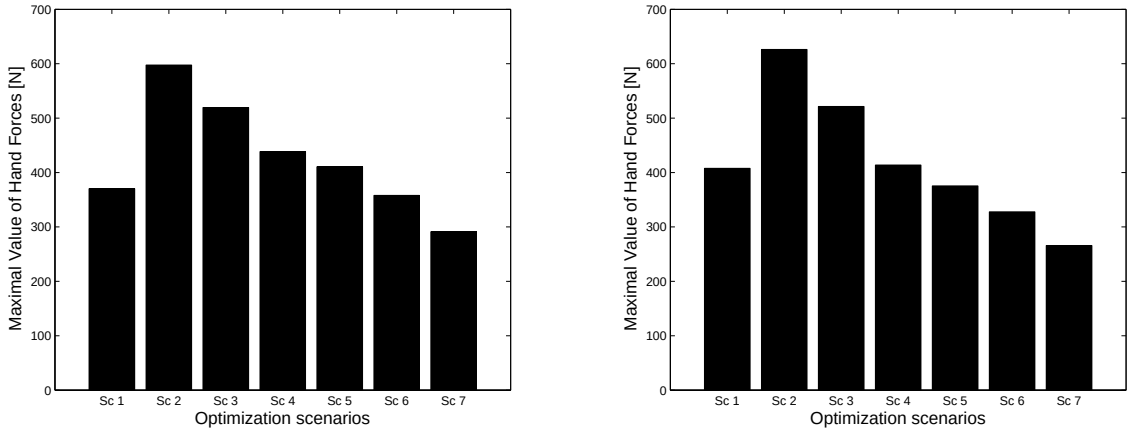

(a) Leading Hand (b) Trailing Hand

Fig. 4. Values of maximal forces underneath the leading(a) and trailing(b) hands.

C. *Torque and force patterns*

Net shoulder and elbow joint torque patterns are shown in Fig. 3. The torque patterns reveal that, for almost all optimization scenarios, the subject relies on bilateral shoulder adductor torque after the seat-off moment, which switches to an abduction torque before the seat-on moment (Fig. 3(c),3(f)). For all scenarios, after the seat-off moment, a trailing shoulder flexion torque is required, this switches to extension torque for scenarios Sc 1, Sc 5-7. The leading shoulder has an extension torque during the transfer, except for Sc 6 and Sc 7 where the flexion torque is needed at the beginning of the motion and switches to extension before seat-on moment (Fig. 3(b),3(e)). An elbow flexion torque is required at the leading upper limb whereas an extension moment is observed at the trailing UL around seat-off. Those torques switch to opposite values before seat-on (Fig. 3(a),3(d)). This kind of behavior has been described in [23].

Fig. 4 represents the maximal peak value of the resultant hand forces obtained with the previous mentioned scenarios Sc (see Section IV-B). As expected, an increase of knee joint torque leads to a reduction of the maximal hand force. The motion of a healthy subject, represented by the first bar, produces a maximal hand force relatively similar to the fifth scenario, and we see that force difference between consecutive scenario tends to decrease while constant knee

joint torque increases.

Those results emphasize the link between the knee stimulation and the maximal contact forces, i.e. the stimulation decreases the contact force of the arms.

CONCLUSION

In this paper, we extend robotics-based technics of motion generation to study the impact of functional electrical stimulation of the knee muscle on the contact forces supported by the arms. The study has proved that the optimization process is well suited for the prediction and the evaluation of SPT task for paraplegic patients. From results presented in this paper, we can conclude that our optimization process is able to predict the knee torque control representing a good trade off (for this specific subject) between the minimization of the maximal hand force and an excessive increase of the lower limb muscular fatigue.

Possibilities for future studies include the influence of some other cost functions, (e.g. minimizing contact forces of the arms) and of some particular environmental constraints such as the position of the chairs and of the initials and final desired sitting posture. As we stated in the Section IV-A, the optimization process has been applied to study only the second phase of the SPT when FES should be applied. Future works will include the history of the motion, i.e. pre-lift and the final stabilization phase. Also, we will generalize the method to other levels of spinal cord injury that can lead for example to a loss of the voluntary control of the hip by the patient. To be as close as possible to paraplegic people, we will also consider zero torque at ankle level. Final validation of our method will consist in a series of experimentation on paraplegic patients and able bodied subjects.

REFERENCES

[1] D. Gagnon, A. M. Koontz, S. J. Mulroy, D. A. Nawoczenski, E. Butler-Forslund, A. Granstrom, S. Nadeau, and M. L. Boninger, "Biomechanics of sitting pivot transfers among individuals with a spinal cord injury: A review of the current knowledge." *Topics in Spinal Cord Injury Rehabilitation*, vol. 15, no. 2, pp. 33–58, 2009.

[2] C. for Spinal Cord Medicine Clinical Practice Guidelines, "Preservation of upper limb function following spinal cord injury: A clinical practice guideline for health-care professionals." *J Spinal Cord Med.*, vol. 28(5), p. 434470, 2005.

[3] A. Kralj and T. Bajd, *Functional electrical stimulation : standing and walking after spinal cord injury.* Boca Raton, Fl: CRC Press, 1989.

[4] D. Popovic and T. Sinkjær, *Control of movement for the physically disabled*. Springer-Verlag London., 2000.

[5] D. Guiraud, T. Stieglitz, K. Koch, J.-L. Divoux, and P. Rabischong, "An implantable neuroprosthesis for standing and walking in paraplegia: 5-year patient follow-up," *J. Neural Eng.*, vol. 3, no. 4, p. 268, 2006.

[6] A. M. Koontz, P. Kankipati, Y.-S. Lin, R. A. Cooper, and M. L. Boninger, "Upper limb kinetic analysis of three sitting pivot wheelchair transfer techniques," *Clin Biomech (Bristol, Avon)*, vol. 26, no. 9, pp. 923–9, 2011.

[7] D. Gagnon, S. Nadeau, L. Noreau, J. J. Eng, and D. Gravel, "Trunk and upper extremity kinematics during sitting pivot transfers performed by individuals with spinal cord injury," *Clin Biomech (Bristol, Avon)*, vol. 23, no. 3, pp. 279–90, 2008.

[8] D. Gagnon, S. Nadeau, L. Noreau, P. Dehail, and D. Gravel, "Quantification of reaction forces during sitting pivot transfers performed by individuals with spinal cord injury," *J Rehabil Med*, vol. 40, no. 6, pp. 468–76, 2008.

[9] Y. Uno, M. Kawato, and R. Suzuki, "Formation and control of optimal trajectory in human multijoint arm movement," *Biological Cybernetics*, vol. 6, no. 2, pp. 89–101, juin 1989.

[10] C. Lin, M. Ayoub, and T. Bernard, "Computer motion simulation for sagittal plane lifting activities," *International Journal of Industrial Ergonomics*, vol. 24, no. 2, pp. 141–155, May 1999.

[11] C. Chang, D. Brown, D. Bloswick, and S. Hsiang, "Biomechanical simulation of manual lifting using space time optimization." *Journal of Biomechanics*, vol. 34, pp. 527–532, 2001.

[12] L. Martin, V. Cahouët, M. Ferry, and F. Fouque, "Optimization model predictions for postural coordination modes," *J Biomech*, vol. 39, no. 1, pp. 170–6, 2006.

[13] I. Bromley, *Tetraplegia and paraplegia: a guide for physiotherapists*, 5th ed. Edinburgh: Churchill Livingstone, 1998.

[14] S.-H. Lee, J. Kim, F. Park, M. Kim, and J. E. Bobrow, "Newton-type algorithms for dynamics-based robot movement optimization," in *IEEE Transactions on robotics*, vol. 21, 2005, pp. 657– 667.

[15] S. Lengagne, A. Kheddar, and E. Yoshida, "Considering floatting contact and un-modeled effects for multi-contact motion generation," in *Workshop on Humanoid Service Robot Navigation in Crowded and Dynamic Environments at the upcoming IEEE Humanoids Conference*, 2011.

[16] S. Lengagne, A. Kheddar, S. Druon, and E. Yoshida, "Emulating human leg impairments and disabilities in walking with humanoid robots," in *IEEE Int. Conf. on RObotics & BIOmimetics*, 2011.

[17] C. De Boor, *A Pratical Guide to Splines*. New York: Springer-Verlag, 1978, vol. 27.

[18] A. Wächter and L. T. Biegler, "On the implementation of a primal-dual interior point filter line search algorithm for large-scale nonlinear programming," *Mathematical Programming*, vol. 106, pp. 22–57, 2006.

[19] A. Murray and P. Larochelle, "A classification scheme for planar 4r, spherical 4r, and spatial rccc linkages to facilitate computer animation," in *ASME Design engineering Technical Conferences*, 1998.

[20] G. Gini, U. Scarfogliero, and M. Folghraiter, "Human-oriented biped robot design: insights into the development of a truly antropomorphic leg," in *IEEE International Conference on Robotics and Automation*, 2007, pp. 2910–2915.

[21] M. Vukobratović and B. Borovac, "Zero-moment point : Thirty five years of its life," *International Journal of Humanoid Robotics*, vol. 1, no. 1, pp. 157–173, 2004.

[22] H. Hirukawa, S. Hattori, K. Harada, S. Kajita, K. Kaneko, F. Kanehiro, K. Fujiwara, and M. Morisawa, "A universal stability criterion of the foot contact of legged robots - adios zmp," in *IEEE International Conference on Robotics and Automation (ICRA).*, may 2006, pp. 1976–1983.

[23] D. Gagnon, S. Nadeau, P. Desjardins, and L. Noreau, "Biomechanical assessment of sitting pivot transfer tasks using a newly developed instrumented transfer system among long-term wheelchair users," *J Biomech*, vol. 41, no. 5, pp. 1104–10, 2008.